Electronic Supplementary Material (ESI) for Chemical Science.

Supplementary Information:

Reconciling Experimental Catalytic Data Stemming from Structure Sensitivity

Xue Zong[1, 2] and Dionisios G. Vlachos[1, 2*]

[1]Department of Chemical and Biomolecular Engineering, 150 Academy St., University of Delaware, Newark, Delaware 19716, United States

[2]Catalysis Center for Energy Innovation, RAPID Manufacturing Institute, and Delaware Energy Institute (DEI), 221 Academy St., University of Delaware, Newark, Delaware 19716, United States

*Corresponding author: vlachos@udel.edu

Supplementary Notes

S1. Definition of Generalized Coordination Number (GCN)

To estimate the GCN of an atom i with n_i nearest neighbors, those neighbors are counted and weighted by their coordination numbers[1], Eq. (1):

$$GCN = \sum_{j=1}^{n_i} \frac{cn(j)n_j}{cn_{max}} \qquad (1)$$

We chose the top site on Pt(111) as an illustration example. There are six atoms in the first layer and three atoms in the second layer. The coordination number is nine and twelve respectively. cn_{max} equals to 12 for an fcc crystal. So the GCN of the top site is thus $GCN = (9 \times 6 + 12 \times 3)/12 = 7.5$.

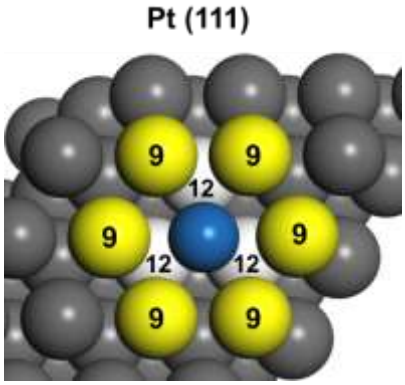

Fig. S1. Top site on Pt(111) surface. *The blue atom denotes the adsorption site. The numbers on the atoms represent the coordination number of the nearest neighbors.*

S2. Predicting Adsorption Energies

The ML model used for predicting adsorption energies was taken from our previous work[2]. Eight features were selected corresponding to the free adsorbate (adsorbate valency of the main element (ME) directly bonded to the metal surface, the number of bonds of the ME in the molecule, the electronegativity of the ME and its nearest neighbor in the molecule, and the molecular weight of the adsorbate) and the adsorption site (GCN, the coordination numbers averaged over the site ensemble, and the number of metal atoms composing the adsorption site). To predict the adsorption energies for each GCN, we first calculated the descriptors related to the free adsorbate. For the adsorption structure descriptors, when a species can adsorb on multiple sites (top, bridge, or hollow), we calculated all adsorption energies and chose the lowest one. For each species, we calculated the errors between the DFT values and the estimates of the ML and the GCN scaling relations. We selected the method with the lowest estimation error for predicting the species energy when varying the structure.

Table S1. Summary of elementary steps, pre-exponential factors (sticking coefficients for adsorptions), temperature exponent, and activation energies in the microkinetic model on Pt(111)*. In the units of the pre-exponential factor, n is the molecularity of the reaction. The pre-factors used on all other structures were the same.*

Elementary Steps	Pre-exponential ($[cm^2/mol]^n s^{-1}$) or Sticking Coefficient (unitless)	Temperature Exponent	Activation Energy (kcal/mol)
$CH_4+*\Leftrightarrow CH_4*$	0.5	0	0
$H_2+2*\Leftrightarrow 2H*$	0.5	0	0
$O_2+2*\Leftrightarrow O_2**$	0.01	0	0
$CO+*\Leftrightarrow CO*$	0.5	0	0
$CO_2+*\Leftrightarrow CO_2*$	0.5	0	0
$H_2O+*\Leftrightarrow H_2O*$	0.5	0	0
$O_2**\Leftrightarrow 2O*$	2.084E+10	1	14.54
$CH_4*+*\Leftrightarrow CH_3*+H*$	8.385E+18	1	24.11
$CH_4*+O*\Leftrightarrow CH_3*+OH*$	8.385E+18	1	34.12
$CH_4*+OH*\Leftrightarrow CH_3*+H_2O*$	8.385E+18	1	25.93
$CH_3*+*\Leftrightarrow CH_2*+H*$	8.385E+18	1	22.16
$CH_3*+O*\Leftrightarrow CH_2*+OH*$	8.385E+18	1	32.70
$CH_3*+OH*\Leftrightarrow CH_2*+H_2O*$	8.385E+18	1	22.82
$CH_2*+*\Leftrightarrow CH*+H*$	8.385E+18	1	6.364
$CH_2*+O*\Leftrightarrow CH*+OH*$	8.385E+18	1	27.27
$CH_2*+OH*\Leftrightarrow CH*+H_2O*$	8.385E+18	1	12.13
$CH*+*\Leftrightarrow C*+H*$	8.385E+18	1	29.65
$CH*+O*\Leftrightarrow C*+OH*$	8.385E+18	1	39.22
$CH*+OH*\Leftrightarrow C*+H_2O*$	8.385E+18	1	19.88
$CHO*+*\Leftrightarrow CH*+O*$	8.385E+18	1	59.40
$CHO*+ *\Leftrightarrow CO*+H*$	8.385E+18	1	8.721
$CHO*+O*\Leftrightarrow CO*+OH*$	8.385E+18	1	14.33
$CHO*+OH*\Leftrightarrow CO*+H_2O*$	8.385E+18	1	0
$COH*+*\Leftrightarrow CO*+H*$	8.385E+18	1	19.28
$COH*+O*\Leftrightarrow CO*+OH*$	8.385E+18	1	10.12
$COH*+OH*\Leftrightarrow CO*+H_2O*$	8.385E+18	1	0
$CO*+*\Leftrightarrow C*+O*$	8.385E+18	1	90.53
$COH*+*\Leftrightarrow C*+OH*$	8.385E+18	1	57.55
$H_2O*+*\Leftrightarrow OH*+H*$	8.385E+18	1	24.76
$OH*+*\Leftrightarrow O*+H*$	8.385E+18	1	27.35
$H_2O*+O*\Leftrightarrow 2OH*$	8.385E+18	1	10.40
$CO_2*+*\Leftrightarrow CO*+O*$	8.385E+18	1	43.37
$COOH*+*\Leftrightarrow CO*+OH*$	8.385E+18	1	15.05
$CHOO*\Leftrightarrow CHO*+O*$	2.084E+10	1	33.73
$COOH*+*\Leftrightarrow CO_2*+H*$	8.385E+18	1	9.869
$COOH*+O*\Leftrightarrow CO_2*+OH*$	8.385E+18	1	2.792

$COOH^*+OH^* \Leftrightarrow CO_2^*+H_2O^*$	8.385E+18	1	5.078
$CHOO^* \Leftrightarrow CO_2^*+H^*$	2.084E+10	1	16.46
$CHOO^*+O^* \Leftrightarrow CO_2^*+OH^*$	8.385E+18	1	25.80
$CHOO^*+OH^* \Leftrightarrow CO_2^*+H_2O^*$	8.385E+18	1	22.92

Table S2. Site occupancy of surface species.

Surface Species	Site Occupancy
CH_4^*	1
CH_3^*	1
CH_2^*	1
CH^*	1
C^*	1
H^*	1
O_2^{**}	2
CO^*	1
CO_2^*	1
H_2O^*	1
O^*	1
OH^*	1
CHO^*	1
COH^*	1
$COOH^*$	1
$CHOO^{**}$	2

Table S3. Lateral interactions (kcal/mol/monolayer) on binding energies. *A linear model is used to estimate binding energies. Blanks denote non-accounted interactions.*

	O^*	H^*	C^*	CH^*	CO^*
O^*	-31				
H^*		-3			
C^*			-15	-15	
CH^*			-15	-15	
CO^*					-15

Table S4. Summary of studies of complete methane oxidation over supported Pt catalysts.

Ref.	Author	Catalyst	Particle Size (nm)	O_2/CH_4	Pt Loading (wt%)	TOF	T (K)	CH_4 Order	O_2 Order	E_{app} (kcal/mol)
[3]	Lee & Vlachos		1.79 ± 0.66	0.2-2.5		0.002-0.7 s^{-1}	553-673	-	1.3	19.49
[4]	Niwa & Murakami			2	0.1	0.117 s^{-1}	573-773	0.9	0.0	21.3
					0.2	0.067 s^{-1}				20.9
					0.5	0.035 s^{-1}				25.2
					0.75	-				25.0
					1.0	0.033 s^{-1}				26.6
					2.0	0.027 s^{-1}				29.3
[5]	Trimm & Lam	Porous		0.7-2.2	0.4	-	773-853	1.0	0.75	44.7
		Non-porous			2.35	-	773-853	1.0	1.0	39.8
[6]	Yao	Pt wire		1-4		0.13 s^{-1} (773 K)	473-773	1.0	-0.6	21
		Pt/Al_2O_3		1-4		0.076 (773 K)	473-773	1.2	-0.6	24
[7]	Cullis & Willatt	Pt/γ-Al_2O_3	13 (2-32)	0.1-10 (0.4)	2.7	0.111 mol/(s·g)	573-673	1.0	0	27.2
[8]	Ma, Trimm & Jiang	Pt/δ-Al_2O_3		0.86-1.3		-	633-733	0.95	-0.17	21.1
[9]	Firth & Holland	Pt/Al_2O_3		<2		-	673-773	1	0	47.6
[10]	Hicks	Pt/Al_2O_3		2.2		0.001 s^{-1}	608	1	0	39.3
						0.001 s^{-1}		1	0	33.6
						0.02 s^{-1}		1	0	33
						0.1 s^{-1}		1	0	29
[11]	Muto	Pt/Al_2O_3		2	0.5	0.075 mmol/(min·g)	723	1	0	25.1
					0.2	0.023 mmol/(min·g)		1	0	20.8
[12]	Chin	Pt/Al_2O_3		< 0.08	0.2	-		0	1	3.8

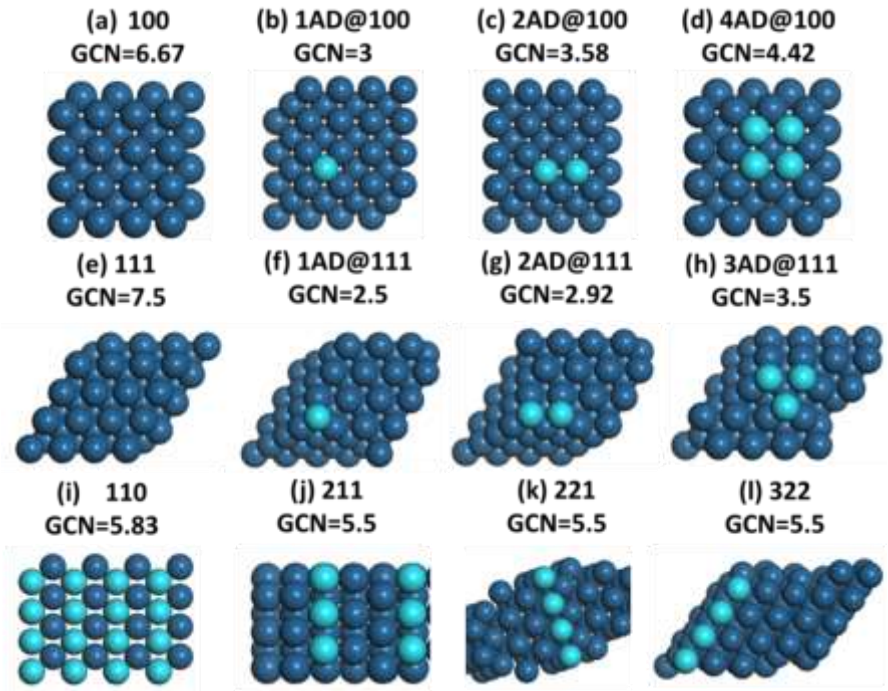

Fig. S2. Structures of Pt extended surfaces with GCNs corresponding to the top site. *Surfaces with n metal adatoms are denoted as nAD@mkl, where mkl are the Miller indices of the plane.*

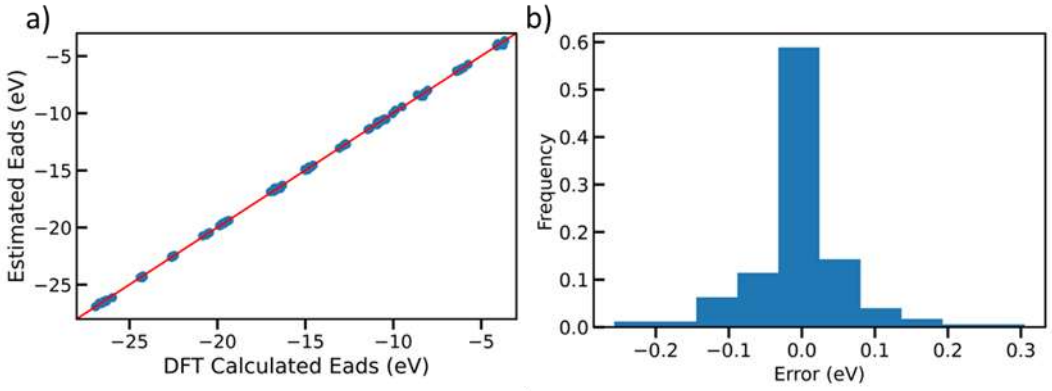

Fig. S3. Summary of errors in estimating adsorption energies for all species. *(a) Parity plot; (b) Histogram of error distributions. Error is defined as the difference between DFT calculated values and estimations from the ML model or GCN scaling relation. See details in Supplementary Estimated_Energy_Errors.xlsx.*

Table S5. Errors in estimating adsorption energies. *MAE represents the mean absolute error in eV. Detailed information of the data used to calculate errors is summarized in Supplementary Estimated_Energy_Errors.xlsx. For each species, adsorption energies on various facets were calculated.*

Species	GCN Relations MAE (eV)	ML Prediction MAE (eV)
CH*	0.068	0.018
C*	0.092	0.139
H_2O*	0.052	0.066
O_2*	0.124	0.031
OH*	0.127	0.057
O*	0.076	0.036
CHOO*	0.113	0.065
CH_4*	0.032	0.026
CH_3*	0.066	0.019
CH_2*	0.130	0.022
H*	0.115	0.059
CO_2*	0.039	0.013
CO*	0.141	0.071
COH*	0.146	0.027
CHO*	0.082	0.028
COOH*	0.065	0.020

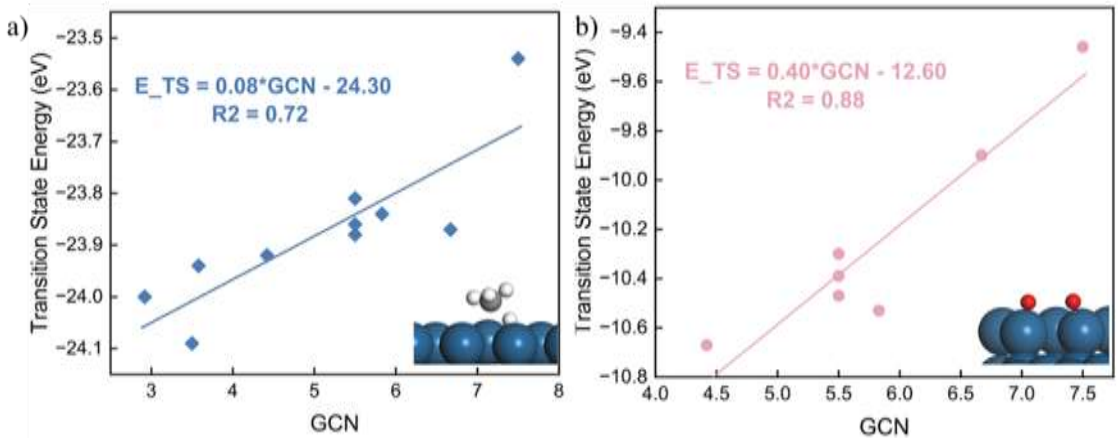

Fig. S4. GCN scaling relations for transition state energies (eV) of two potential rate-determining steps. *a) CH_4 first dehydrogenation; b) O_2 dissociation. The configurations of transition states are shown as insets. See data in Table S6.*

Table S6. Transition state energies for potential rate-determining steps. *E_TS (CH_4) represents the CH_4 first dehydrogenation reaction, and E_TS (O_2) represents the O_2 dissociative adsorption. At least two bridge sites are required to stabilize O_2 dissociative products (two O* species), so there is no data for O_2 dissociation on facets with a few adatoms (2AD@111, 2AD@100, and 3AD@111).*

Facet	GCN	E_TS (CH_4)	E_TS (O_2)
111	7.5	-23.54	-9.46
100	6.67	-23.87	-9.90

110	5.83	-23.84	-10.53
211	5.5	-23.88	-10.30
221	5.5	-23.81	-10.47
322	5.5	-23.86	-10.39
2AD@111	2.92	-24.00	-
2AD@100	3.58	-23.94	-
3AD@111	3.5	-24.09	-
4AD@100	4.42	-23.92	-10.67

Table S7. Brønsted-Evans-Polanyi (BEP) correlation parameters. *The reactions used for developing BEPs were in the cleavage direction. C-H and O-H represent dehydrogenation reactions, while C-C and C-O represent cracking reactions. C-H abstraction by O* and OH* are denoted as C-H + O and C-H + OH respectively, with same notation applied to O-H abstraction.*

Correlation	Slope	Intercept (kcal/mol)	Reference
C-H	1.02	24.38	[13]
C-O	0.84	43.01	
C-OH	0.69	32.89	
O-H	0.86	12.88	
C-H + O	0.94	30.82	[14]
C-H + OH	0.68	25.3	
O-H + O	0.65	3.68	
O-H + OH	0.02	0.46	

Table S8. Summary of various models and their kinetic results. *E_{app} represents the apparent activation energy in kcal/mol. 111-DFT represents the first principles-based MKM on Pt(111). The 111-BEP model replaces the activation barriers of non-RDS reactions of the 111-DFT model with BEP estimated values. The GCN-7.5 model employs the new methodology at GCN=7.5 which corresponds to Pt(111).*

Model	TOF (s^{-1})	Coverages (ML)	Rate-determining step	CH_4 order	O_2 order	E_{app} (kcal/mol)
111-DFT	1.95	O* (0.48) * (0.52)	CH_4*+*=CH_3*+H*	1	-0.1	13.9
111-BEP	17.3	O* (0.48) * (0.51)	CH_4*+OH*=CH_3*+H_2O*	1.5	0.2	10.2
GCN-7.5	45.2	O* (0.42) * (0.58)	CH_4*+*=CH_3*+H*	1.1	0.0	10.8

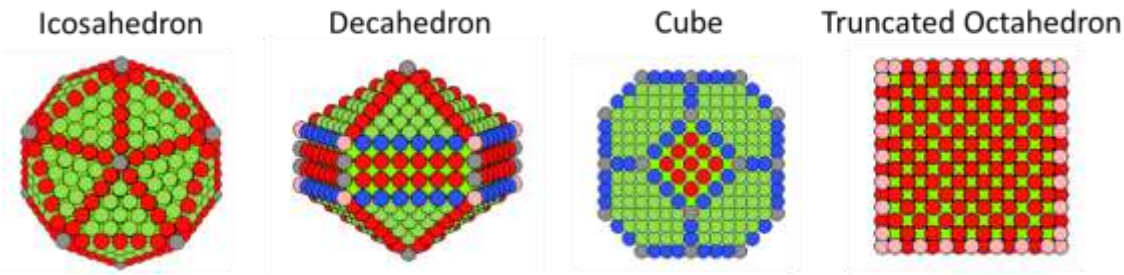

Fig. S5. Pt nanoparticles with various morphologies. *Different colors represent atoms with different coordination environments (see Table S9).*

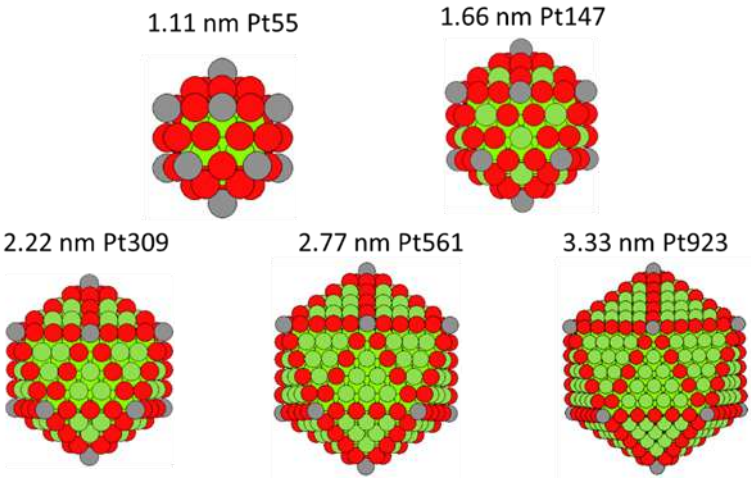

Fig. S6. Pt icosahedron particles of different sizes. *Different colors correspond to atoms with different coordination environments (see Table S10).*

Table S9. GCN distributions for Pt nanoparticles of different shapes.

GCN	Icosahedron	Decahedron	Octahedron	Cube
3.1667				0.0408
3.3333		0.0284		
3.6667				0.1020
4.25		0.0284	0.0615	
4.3333	0.0331	0.0057		
5.0833		0.0568	0.0615	
5.25			0.1231	
5.3333		0.1136	0.0615	
5.75		0.0284		
5.833				0.2449
6	0.1657	0.0284		
6.3333	0.2486	0.1136		

6.4167		0.0568		
6.5			0.0615	
6.5833		0.1136	0.0615	
6.6667			0.0154	0.6122
6.9167			0.1231	
7		0.0568		
7.1667	0.1657	0.1136	0.1846	
7.3333	0.3315	0.1705		
7.5	0.0552	0.0852	0.2462	

Table S10. GCN distributions for icosahedron nanoparticles of different diameters.

Diameter / GCN	1.11 nm	1.66 nm	2.22 nm	2.77 nm	3.33 nm
4.33	0.29	0.13	0.07	0.04	0.03
5.67	0.71				
6		0.65	0.37	0.24	0.17
6.33			0.19	0.24	0.25
7		0.22			
7.17			0.37	0.24	0.16
7.33				0.24	0.33
7.5					0.06

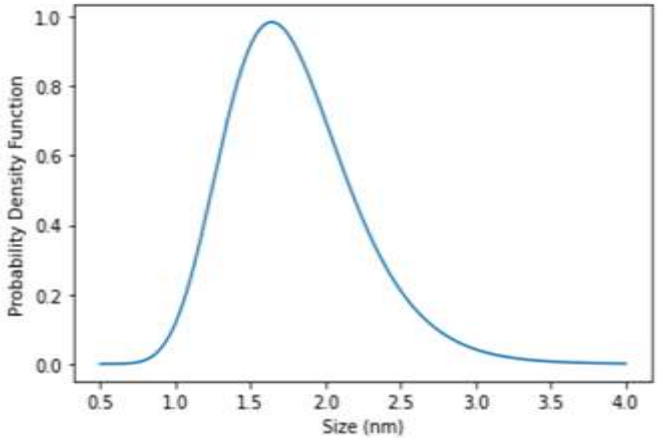

Fig. S7. *Probability density function estimated from experimental particle size reported by Lee et al*[3]*.*

Table S11. *Estimated probability for given particle size range from the probability density function. TOF @ size denotes the TOF calculated for icosahedral nanoparticles at given diameters. The results are taken from the manuscript Fig. 5b.*

Particle Size Range (nm)	Probability	TOF (s^{-1}) @ size (nm)
1.0-1.2	0.050	3.46 @ 1.11
1.5-1.7	0.193	12.8 @ 1.66
2.1-2.3	0.094	181 @ 2.22
2.6-2.8	0.023	118 @ 2.77
3.2-3.4	0.003	95 @ 3.33

References

1 F. Calle-Vallejo, J. I. Martínez, J. M. García-Lastra, P. Sautet and D. Loffreda, *Angew. Chem. Int. Ed.*, 2014, **53**, 8316–8319.
2 X. Zong and D. G. Vlachos, *J. Chem. Inf. Model.*, 2022, **62**, 4361–4368.
3 G. Lee, W. Zheng, K. A. Goulas, I. C. Lee and D. G. Vlachos, *Ind. Eng. Chem. Res.*, 2019, **58**, 17718–17726.
4 M. Niwa, K. Awano and Y. Murakami, *Appl. Catal.*, 1983, **7**, 317–325.
5 D. L. Trimm and C.-W. Lam, *Chem. Eng. Sci.*, 1980, **35**, 1405–1413.
6 Y.-F. Y. Yao, *Ind. Eng. Chem. Prod. Res. Dev.* 1980, **19,** 293–298.
7 C. F. Cullis and B. M. Willatt, *J. Catal.*, 1983, **83**, 267–285.
8 L. Ma, D. L. Trimm and C. Jiang, *Appl. Catal. A: General*, 1996, **138**, 275–283.
9 J. G. Firth and H. B. Holland, *Trans. Faraday Soc.*, 1969, **65**, 1121.
10 R. F. Hicks, H. Qi, M. L. Young and R. G. Lee, *J. Catal.*, 1990, **122**, 280–294.
11 K. Otto, *Langmuir*, 1989, **5**, 1364–1369.
12 Y.-H. Chin, C. Buda, M. Neurock and E. Iglesia, *J. Am. Chem. Soc.*, 2011, **133**, 15958–15978.
13 J. E. Sutton and D. G. Vlachos, *ACS Catal.*, 2012, **2**, 1624–1634.
14 J. E. Sutton, P. Panagiotopoulou, X. E. Verykios and D. G. Vlachos, *J. Phys. Chem. C*, 2013, **117**, 4691–4706.